

Effects of anthropogenic heat on ozone air quality in a megacity

Young-Hee Ryu^a, Jong-Jin Baik^{a,*}, Sang-Hyun Lee^b

^a School of Earth and Environmental Sciences, Seoul National University, Seoul 151-742, Republic of Korea

^b Department of Atmospheric Science, Kongju National University, Gongju 314-701, Republic of Korea



HIGHLIGHTS

- The effects of anthropogenic heat on ozone (O_3) air quality in the Seoul metropolitan area are examined.
- Due to the modified local meteorology by anthropogenic heat, O_3 concentration increases in the urban area.
- In the deepened boundary layer, the chemical loss of O_3 by NO is reduced because of the decrease in NO_x concentration.
- By the inward flow of urban-breeze circulation, O_3 -rich air in the surrounding rural area is advected over the urban area.

ARTICLE INFO

Article history:

Received 12 March 2013

Received in revised form

20 July 2013

Accepted 25 July 2013

Keywords:

Anthropogenic heat

Ozone

Air quality

Urban heat island

Urban breeze

Sea/land breeze

Seoul

ABSTRACT

Anthropogenic heat released into the atmosphere in urban areas affects the characteristics/structures of boundary layer and local circulation and thus can affect local air quality. In this study, the effects of anthropogenic heat on ozone (O_3) air quality in the Seoul metropolitan area, Republic of Korea, are examined using the Community Multiscale Air Quality (CMAQ) model coupled with the Weather Research and Forecasting (WRF) model. The release of anthropogenic heat is found to increase O_3 concentration by 3.8 ppb in the urban area, and this effect is larger in the nighttime (5.3 ppb) than in the daytime (2.4 ppb). As stronger anthropogenic heat is released, the urban boundary layer becomes deeper and NO_x concentration becomes lower due to the dilution. The decrease in NO_x concentration causes the chemical loss of O_3 by the reaction with NO to be reduced. In addition to the enhanced net chemical production of O_3 in the deepened urban boundary layer, the strengthened urban-breeze circulation by anthropogenic heat contributes to an increase in O_3 concentration in the urban area. The O_3 -rich air in the surroundings of Seoul, where biogenic volatile organic compound (BVOC) emissions are high and NO_x emissions are low, is brought into the urban area by the urban breeze. Moreover, in the daytime, the advection of oxidant products of BVOCs by the urban breeze contributes to an enhanced chemical production of O_3 in the urban area. Anthropogenic heat also modifies the sea/land-breeze circulations, which, in turn, is found to influence O_3 concentration in the urban area.

© 2013 Elsevier Ltd. All rights reserved.

1. Introduction

Anthropogenic heat is the heat released as a by-product of fuel combustion and/or energy consumption (Oke et al., 1991). It has been known that anthropogenic heat can significantly influence the urban thermal environment. For example, it has been reported that the addition of anthropogenic heat can increase the near-surface air temperature by approximately 1–2 °C in summer and 2–3 °C in winter (e.g., Ichinose et al., 1999; Kondo and Kikegawa, 2003; Fan and Sailor, 2005; Ohashi et al., 2007). The effects of anthropogenic heat have been shown to be more significant in the

nighttime than in the daytime even though anthropogenic heat intensity is generally stronger in the daytime (e.g., Ichinose et al., 1999; Fan and Sailor, 2005; Chen et al., 2009). In addition, it has been reported that anthropogenic heat can modify the characteristics/structures of the atmospheric boundary layer (ABL) in urban areas (e.g., Ichinose et al., 1999; Fan and Sailor, 2005; Makar et al., 2006; Lin et al., 2008; Chen et al., 2009). For example, Chen et al. (2009) showed that the urban boundary layer becomes more turbulent and unstable when anthropogenic heat is released, especially in the morning and evening. Because the release of anthropogenic heat increases air temperature in urban areas, anthropogenic heat can also modify local circulation. Sang et al. (2000) and Chen et al. (2009) showed that anthropogenic heat strengthens urban-breeze circulations that are induced by urban heat islands (UHIs) (also called UHI circulations). Lin et al. (2008)

* Corresponding author. Tel.: +82 2 880 6990; fax: +82 2 883 4972.

E-mail address: jjbaik@snu.ac.kr (J.-J. Baik).

reported that, in northern Taiwan, anthropogenic heat strengthens the sea breeze in the daytime and weakens the land breeze in the nighttime.

Since air pollution is strongly associated with the ABL structure and local circulation, it is expected that anthropogenic heat can have considerable effects on air pollution. However, to the authors' knowledge, there is no comprehensive study that examines the effects of anthropogenic heat on air pollution. The purpose of the present study is to investigate the effects of anthropogenic heat on ozone air quality in the summer in the Seoul metropolitan area. For this, a high ozone episode on 24 June 2010 is examined in which elevated O₃ levels were observed to exceed 100 ppb under fair weather conditions and an air quality model is employed to simulate the case. For the same episode and study area, Ryu et al. (2013) examined the effects of urban-modified boundary layer and local circulation on ozone air quality. They showed that O₃ concentration in the urban area increases owing to urban land-surface forcing. Based on the current understanding of the impacts of urban land-surface forcing on ozone air quality, this study aims to address how the boundary layer and local circulation modified by anthropogenic heat affect ozone air quality and how the degree of this effect changes as anthropogenic heat intensity changes. To pursue this goal, gridded anthropogenic heat data established by Lee et al. (2009) are used and several types of anthropogenic heat release scenarios are considered.

In section 2, an experimental setup is briefly described and the model is validated against observations. Simulation results are presented and discussed in section 3. Summary and conclusions are given in section 4.

2. Model, experimental setup, and validation

2.1. Model and experimental setup

In this study, the Community Multiscale Air Quality (CMAQ) model coupled with the Weather Research and Forecasting (WRF) model in an offline is employed. The output of the WRF model simulation is used as meteorological input of the CMAQ model simulation. Fig. 1a shows the domain configuration of the CMAQ model simulation. The horizontal grid sizes of the three domains are 9 km, 3 km, and 1 km. The model is integrated for 72 h starting from 0900 LT (= UTC + 9 h) 22 June 2010, and the simulation data of 24 June 2010 are used for analyses. The experimental setup for the meteorological and air quality simulations in the present study is the same as that used in Ryu and Baik (2013) and Ryu et al. (2013), except for the setup conditions of anthropogenic heat. In the two previous studies, the intensity and temporal profiles of released anthropogenic heat were prescribed depending on the type of urban land use/land cover (LULC). The present study uses gridded anthropogenic heat data established by Lee et al. (2009), which were estimated for base year of 2002 and have spatial and temporal variations with resolutions of 0.01° in space and an hour in time, respectively. To estimate anthropogenic heat release, four energy sectors of electricity, transportation, point sources, and area sources are separately considered. For the energy sectors, the annual anthropogenic heat release is estimated based on the energy consumption statistics data and then is spatially distributed using spatial surrogates such as population density, road length and lane, and land use distribution. Using observed and statistical data, monthly and hourly allocating profiles for all the sources are applied. Lee et al. (2009) showed that the diurnal variations of the anthropogenic heat fluxes averaged over summer and winter seasons in the study area are similar to those found in US cities

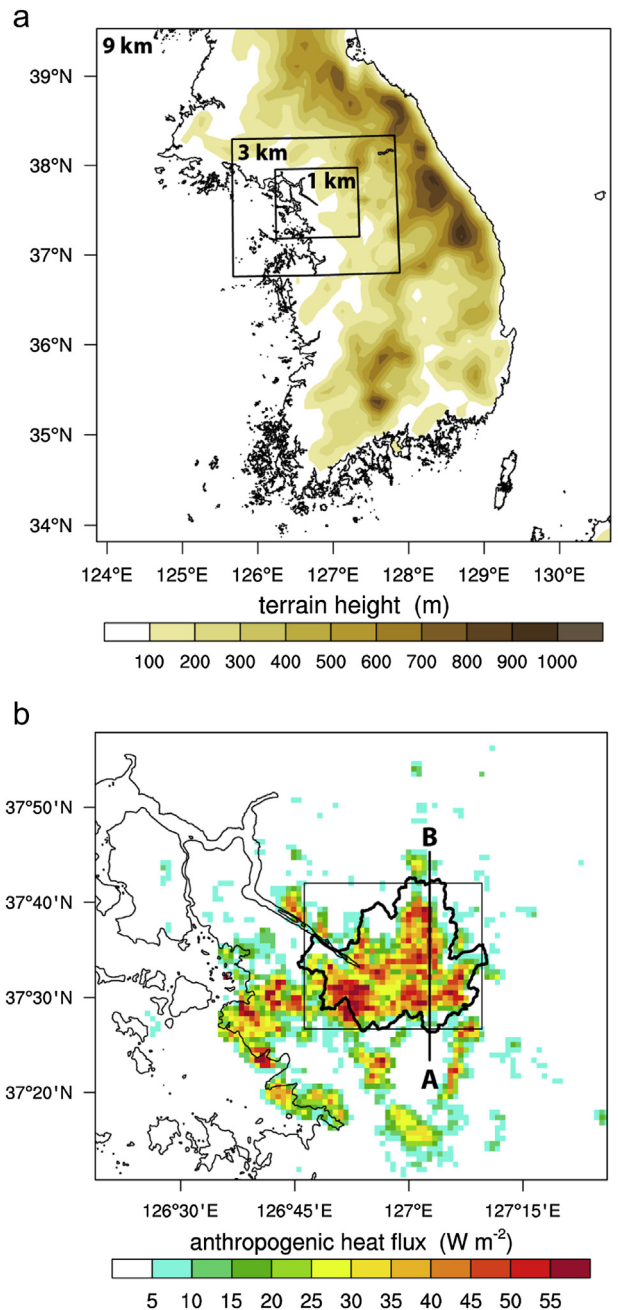


Fig. 1. (a) Domain configuration of the CMAQ model simulation (after Ryu et al., 2013). (b) Distribution of the daily-averaged anthropogenic heat flux on 24 June 2010 in the innermost domain. The thick line indicates the administrative boundaries of Seoul, and the rectangle indicates the urban analysis area.

(Sailor and Lu, 2004) with different magnitudes. Note that in the WRF model that is coupled with the Seoul National University Urban Canopy Model (Ryu et al., 2011) anthropogenic heat is added into the urban canyon in the canopy model and that in the WRF model anthropogenic heat release is considered in all the three domains. Fig. 1b shows the spatial distribution of daily-averaged anthropogenic heat flux in the innermost domain. The anthropogenic heat intensity is particularly strong in the southwestern region of Seoul where industrial complexes are located and population density is high. Note that the distribution of anthropogenic heat release generally coincides with that of NO_x emission [see Fig. 1c in Ryu et al. (2013)].

To examine the effects of anthropogenic heat on local meteorology and air quality, four pairs of meteorological and air quality simulations are performed: simulations without anthropogenic heat (AHF0), simulations with a baseline anthropogenic heat (AHF1), simulations with doubled anthropogenic heat (AHF2), and simulations with quadrupled anthropogenic heat (AHF4). In all air quality simulations, the same anthropogenic and biogenic emissions are used. Fig. 2a shows the diurnal variations of anthropogenic heat flux averaged over the urban analysis area (marked by a rectangle in Fig. 1b) in the AHF1, AHF2, and AHF4 simulations. In all analyses in this study, only the grids corresponding to the urban LULC [see Fig. 1b in Ryu et al. (2013)] in the urban analysis area are used when taking an average. In the three simulations, the anthropogenic heat intensity is stronger in the daytime than in the nighttime and has one peak in the morning and another in the evening. The anthropogenic heat intensity in the AHF4 simulation seems quite strong, but the intensity is reasonably strong as compared with intensities reported in previous studies. For instance, Ichinose et al. (1999) documented that in a highly built-up area in central Tokyo the anthropogenic heat flux is around 200 W m^{-2} during the daytime in summer. In addition, under extreme weather conditions (for example, heat-wave conditions) or future urban warming conditions the anthropogenic heat intensity can be expected to be as strong as that in the AHF4 simulation.

2.2. Validation

In Ryu and Baik (2013) and Ryu et al. (2013), results of the WRF model and CMAQ model simulations were validated against observations for the same high O_3 episode. In the present study, results of the baseline simulation (AHF1 simulation) are found to be similar to those obtained in the previous studies. Table 1 presents statistics that evaluate performance in reproducing near-surface air temperature and O_3 concentration. Detailed information about the stations/sites whose observation data are compared with the simulation data is given in Ryu and Baik (2013) and Ryu et al. (2013). The near-surface air temperature is simulated reasonably well with a mean bias error of 0.6°C and a root-mean-square error of 1.5°C . The performance statistics for O_3 concentration obtained in the present study are similar to those obtained in Ryu et al. (2013), ensuring good performance in reproducing O_3 concentration.

3. Results and discussion

Anthropogenic heat can influence the surface energy balance in urban areas. In particular, it can contribute greatly to an increase in sensible heat. Fig. 2b shows the diurnal variations of sensible heat flux averaged over the urban analysis area in the AHF0, AHF1, AHF2, and AHF4 simulations. As expected, the addition of

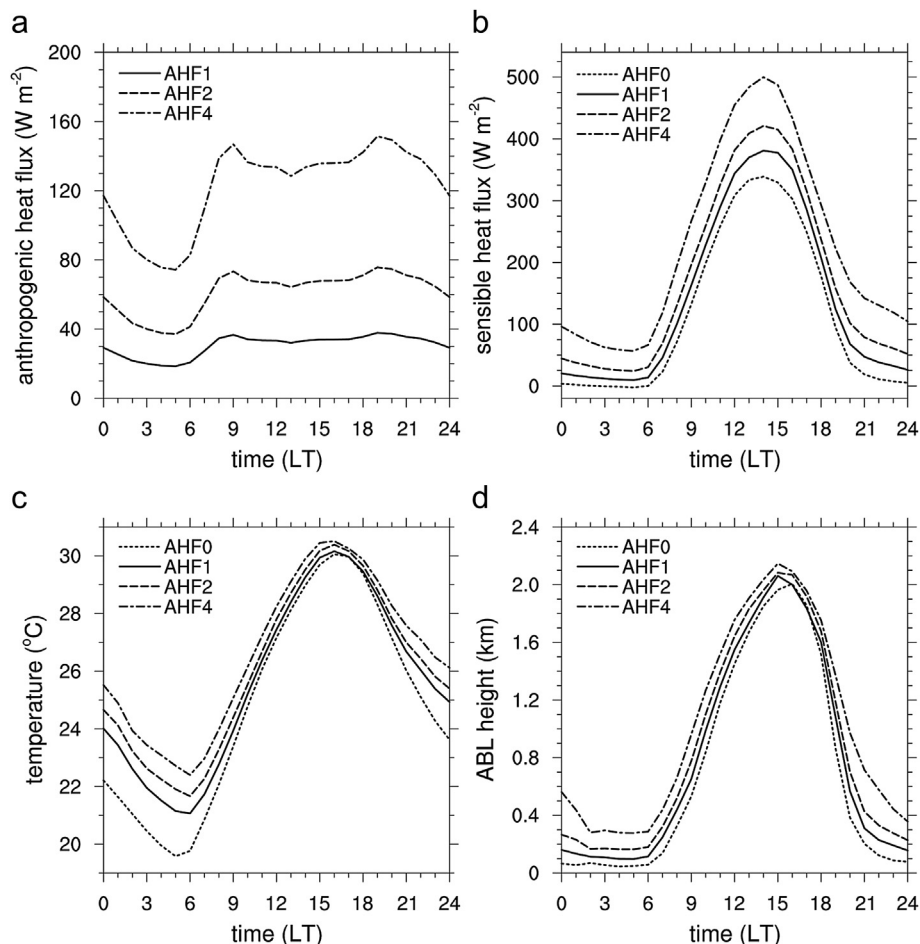


Fig. 2. Diurnal variations of (a) anthropogenic heat flux, (b) sensible heat flux, (c) near-surface air temperature, and (d) atmospheric boundary layer (ABL) height averaged over the urban analysis area in the AHF0, AHF1, AHF2, and AHF4 simulations. The description of the four simulations is given in the text.

Table 1

Performance statistics for near-surface air temperature and O₃ concentration. The number of observation sites used for calculating the performance statistics for near-surface temperature (near-surface O₃ concentration) is 12 (71). The MBE and RMSE stand for the mean bias error and root-mean-square-error, respectively. The MNBE and MNGE stand for the mean normalized bias error and mean normalized gross error, respectively.

	Metric	Performance statistic
Temperature	MBE (°C)	0.6
	RMSE (°C)	1.5
O ₃ concentration	MNBE (%)	7.4
	MNGE (%)	25.8
	MBE (ppb)	4.2
	RMSE (ppb)	20.3

anthropogenic heat and increases in anthropogenic heat intensity cause increases in sensible heat flux. Consequently, the near-surface air temperature and the ABL height increase as anthropogenic heat intensity increases as can be seen in Fig. 2c and d, respectively. The effect of anthropogenic heat on temperature is more significant in the nighttime than in the daytime as previously demonstrated in a number of studies (e.g., Ichinose et al., 1999; Fan and Sailor, 2005; Chen et al., 2009). For example, the near-surface air temperature at 0500 LT (1500 LT) is 3.1 °C (0.8 °C) higher in the AHF4 simulation than in the AHF0 simulation. The difference in ABL height between the AHF0 and AHF4 simulations is large in the morning and evening, exhibiting large differences of 429 m at 0900 LT and of 588 m at 2000 LT. This feature is likely associated with the strong anthropogenic heat intensity in the morning and evening hours (Fig. 2a). On average, the difference in ABL height between the two simulations is larger in the nighttime (362 m) than in the daytime (278 m). As in Ryu et al. (2013), the nighttime average is taken over 0000–0500 LT and 2000–2400 LT and the daytime average is taken over 0600–1900 LT. These results are consistent with the findings of Fan and Sailor (2005) and Chen et al. (2009).

Fig. 3 shows the diurnal variations of near-surface O₃ and NO_x (= NO + NO₂) concentrations averaged over the urban analysis area in the AHF0, AHF1, AHF2, and AHF4 simulations. When anthropogenic heat is released, near-surface O₃ concentration increases by 3.8 ppb on average (difference between the AHF1 and AHF0 simulations). The difference in O₃ concentration between the two simulations is on average 2.4 ppb in the daytime and 5.3 ppb in the nighttime. The O₃ and NO_x concentrations vary depending on anthropogenic heat intensity. For example, at 0500 LT (1500 LT), O₃ concentration is 8.7 ppb (5.9 ppb) higher and NO_x concentration is 26.1 ppb (5.7 ppb) lower in the AHF4 simulation than in the AHF0 simulation. The large difference in NO_x concentration at 0700 LT among the simulations is likely due to the high NO_x emissions during the morning rush hours when the difference in ABL height among the simulations is quite large. As demonstrated in Sarrat et al. (2006) and Ryu et al. (2013), the increase in O₃ concentration in the nighttime is most likely attributed to the increase in ABL height and thus the decrease in NO_x concentration due to the dilution. Even though the dilution also decreases O₃ concentration, O₃ concentration ultimately increases because the chemical loss of O₃ by the reaction with NO (referred to as NO_x titration) is reduced in the deepened ABL. It should be noted that the anthropogenic heat release used in this study is estimated based on the energy consumption statistics data on 2002. Even though there could be uncertainties in anthropogenic heat release arising from the year gap, such uncertainties would not change our findings because the anthropogenic heat shows consistent effects on ozone air quality both in the nighttime and in the daytime even though its intensity varies under the four scenarios.

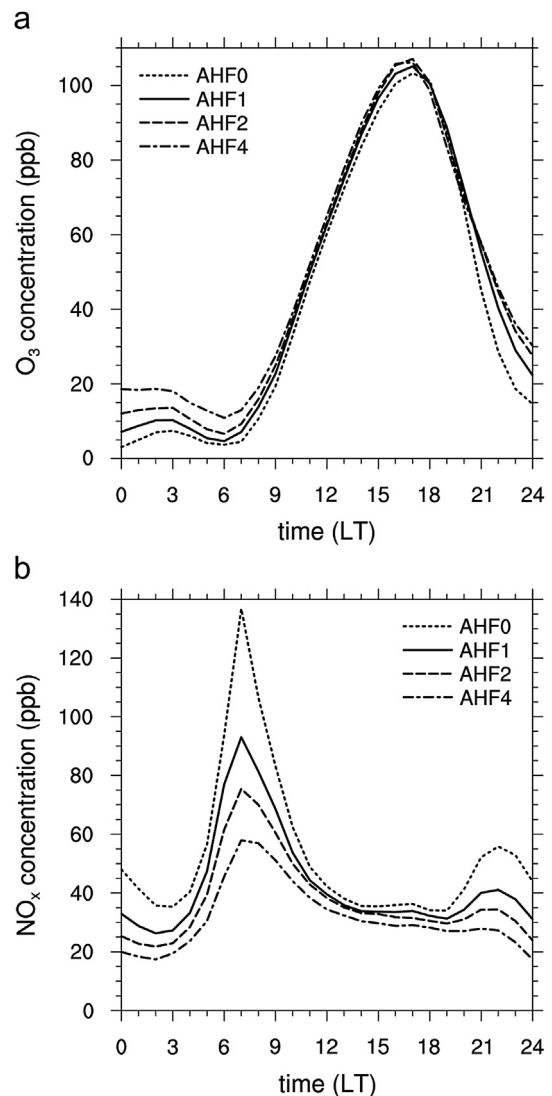


Fig. 3. Diurnal variations of near-surface (a) O₃ and (b) NO_x concentrations averaged over the urban analysis area in the AHF0, AHF1, AHF2, and AHF4 simulations.

Moreover, anthropogenic heat modifies local circulation in the nighttime. Fig. 4 shows the near-surface O₃ concentration and wind fields at 0500 LT in the AHF0, AHF1, AHF2, and AHF4 simulations. At 0500 LT, the urban-breeze circulation develops well in all the simulations although its intensity varies considerably among the simulations. It is seen that as anthropogenic heat intensity increases the intensity of urban-breeze circulation increases because of the increase in temperature difference between the urban area and the surroundings (i.e., increase in UHI intensity). As seen in the area-averaged concentration (Fig. 3a), O₃ concentration in the urban area is lowest in the simulation without anthropogenic heat (AHF0 simulation) and highest in the simulation with the strongest anthropogenic heat intensity (AHF4 simulation). The differences in wind and in O₃ concentration between the AHF1, AHF2, and AHF4 simulations and the AHF0 simulation over Seoul are shown in the small figures on the upper left corners in Fig. 4b–d. The urban-breeze circulation modified by anthropogenic heat can cause an increase in O₃ concentration. The inward flow toward the city center that is part of the urban-breeze circulation brings the O₃-rich air into the urban area from the surroundings where O₃ concentration is higher due to the

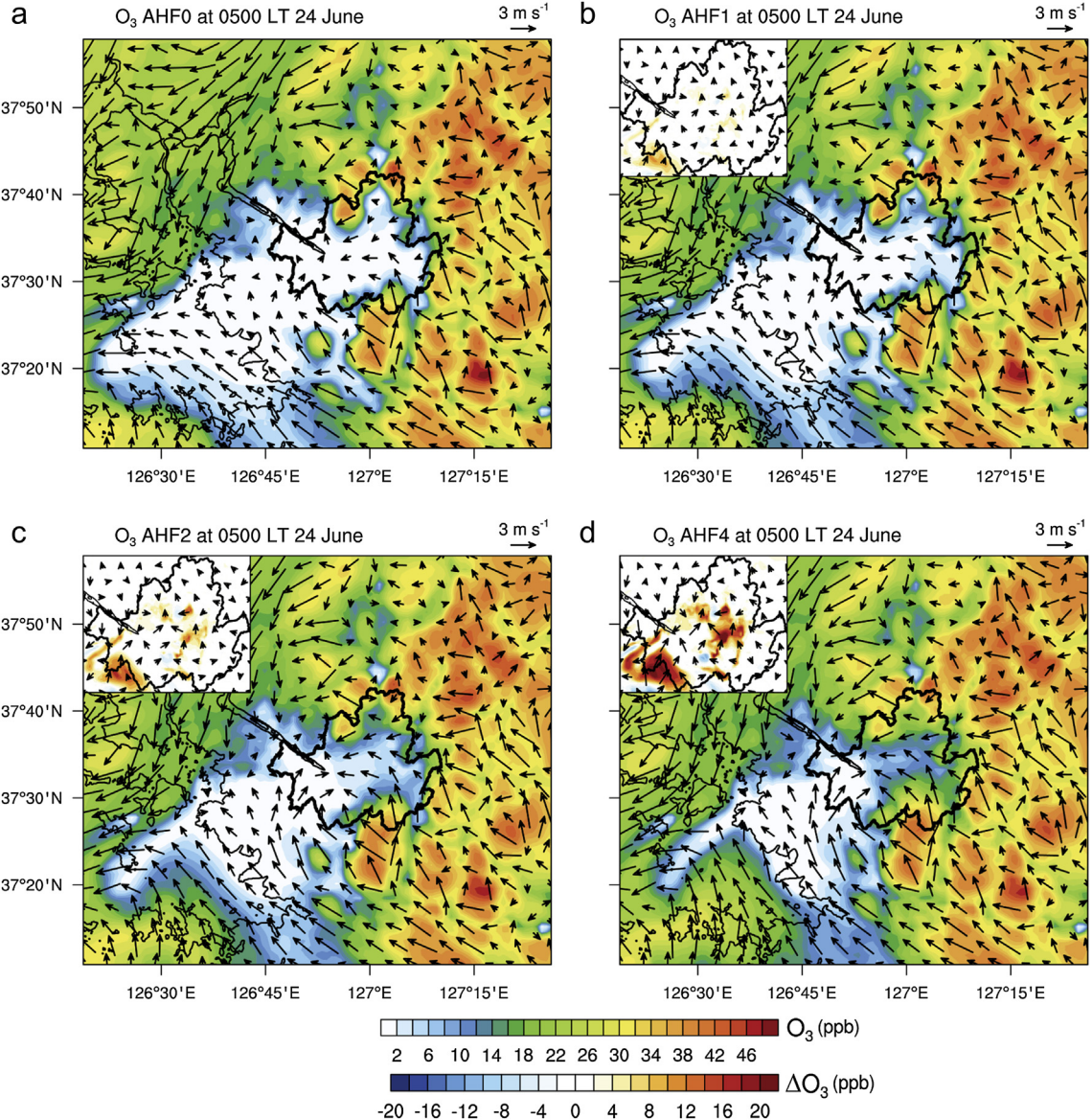


Fig. 4. Horizontal distributions of O_3 concentration and wind at the lowest model level at 0500 LT 24 June 2010 in the (a) AHF0, (b) AHF1, (c) AHF2, and (d) AHF4 simulations. The small figures on the upper left corners in (b)–(d) show differences in wind and O_3 concentration fields between the AHF1, AHF2, and AHF4 simulations and the AHF0 simulation (i.e., each simulation minus AHF0 simulation). The wind vector scale for the differential wind is the same as the scale for the wind at the lowest model level. The color bar for the differential O_3 concentration (ΔO_3) is given in the second color bar.

much lower NO_x emissions than that in the urban area. Because the urban-breeze circulation becomes stronger as anthropogenic heat intensity is stronger, O_3 concentration in the urban area increases correspondingly.

To examine the relative importance of the ABL and local circulation modified by anthropogenic heat, an Integrated Process Rate (IPR) analysis (Gipson, 1999) is performed as done in Ryu et al. (2013). Fig. 5 shows the vertical profiles of O_3 concentration and contributions of individual physical/chemical processes to the change in O_3 concentration for the period from 0100 to 0500 LT, during which the change in O_3 concentration with time is relatively small, in the AHF0 and AHF4 simulations. Note that the area-averaged contribution of each process is normalized by the area-averaged O_3 concentration to compare each contribution in the simulations. While O_3 concentration in the AHF0 simulation exhibits a relatively large vertical gradient, which implies an

enhanced O_3 loss near the surface, O_3 concentration in the AHF4 simulation exhibits a relatively small vertical gradient. From the IPR analysis results, it is found that the main reason for the removal of O_3 in the nighttime is the chemical loss of O_3 . Because NO_x concentration is higher (Fig. 3b) in the shallower ABL (Fig. 2d), the effect of NO_x titration in the AHF0 simulation is larger than that in the AHF4 simulation. In both simulations, the removal of O_3 is compensated by a downward diffusion, but the degree of diffusion is larger in the AHF0 simulation than in the AHF4 simulation because of the larger vertical gradient. Surprisingly, the contribution of the advection process is larger in the AHF0 simulation than in the AHF4 simulation. This is likely due to the larger horizontal gradient of O_3 concentration between the urban area and the surroundings in the AHF0 simulation than in the AHF4 simulation. Because the O_3 -rich air in the surroundings is advected over the urban area where O_3 concentration is much

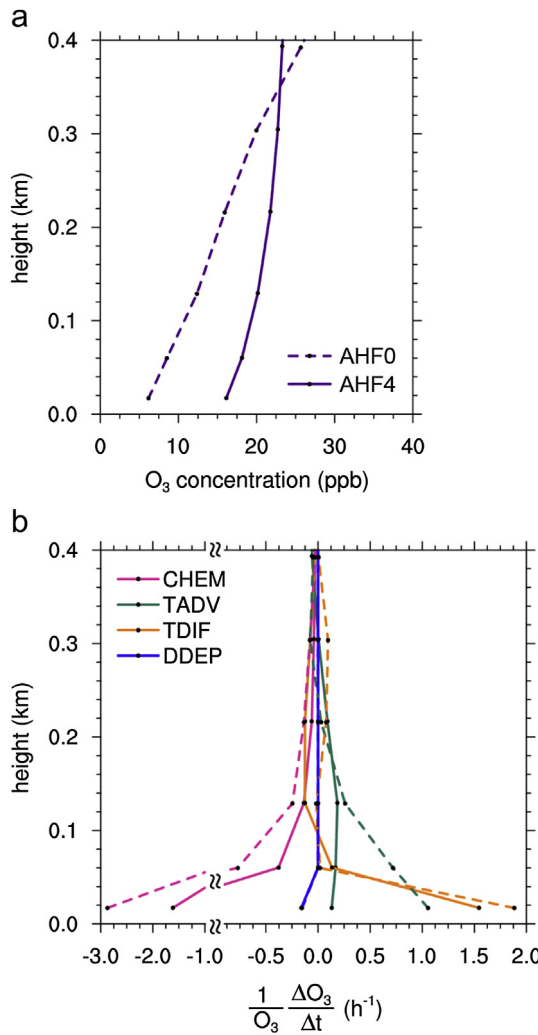


Fig. 5. Vertical profiles of area-averaged (a) O₃ concentration and (b) contributions of individual processes normalized by area-averaged O₃ concentration for the period of 0100–0500 LT 24 June 2010 in the AHF0 (dashed lines) and AHF4 (solid lines) simulations. The area average is taken over the urban analysis area. The CHEM, TADV, TDIF, and DDEP refer to the chemical, advection (horizontal and vertical), diffusion (horizontal and vertical), and dry deposition processes, respectively.

lower due to NO_x titration, the contribution of the advection process itself can be relatively large in the AHF0 simulation. These results indicate that even though O₃ is advected considerably over the urban area from the surroundings, O₃ concentration greatly decreases when NO_x concentration is high in the shallow ABL. In short, the main reason for the increase in O₃ concentration with increasing anthropogenic heat intensity is that the chemical loss of O₃ by the reaction with NO is reduced in the deepened urban boundary layer.

Interestingly, the advection of NO_x, one of the O₃ precursors, over the Yellow Sea (the sea to the west of the study area) in the AHF0 simulation is enhanced in the nighttime as compared with that in the other simulations. Note that the prevailing wind direction of land breeze in the nighttime and early morning is easterly in the study area. Because O₃ and NO_x concentrations are anti-correlated in the nighttime (not shown), the enhanced advection of NO_x over the sea can be inferred from the low O₃ concentration over the sea in the AHF0 simulation (Fig. 4a). Due to the stronger urban-breeze circulation that develops when anthropogenic heat intensity is stronger, more pollutants converge toward the urban

area. For the weaker urban-breeze circulation, on the other hand, more pollutants can be advected toward the surroundings (e.g., the sea). The advection of NO_x and other O₃ precursors in the nighttime can affect daytime O₃ production over the sea. This issue is addressed later in this section.

In the daytime, even though the difference in O₃ concentration among the simulations is not as significant as that in the nighttime, the difference in O₃ concentration is relatively large during 1500–1700 LT (Fig. 3a). Fig. 6 shows the vertical profiles of O₃ concentration and contributions of individual physical/chemical processes to the change in O₃ concentration for the period from 1100 to 1500 LT in the AHF0 and AHF4 simulations. In the ABL, O₃ concentration is higher when the strong anthropogenic heat is released than when no anthropogenic heat is released (Fig. 6a). As in the nighttime, the reduced chemical loss of O₃ near the surface causes an increase in O₃ concentration in the AHF4 simulation (Fig. 6b). As pointed out in Ryu et al. (2013), the upward transport of O₃ precursors into the upper ABL by the enhanced upward motion and vigorous mixing in the deepened urban boundary layer also contributes to the enhanced chemical production of O₃ in the upper ABL in the AHF4 simulation.

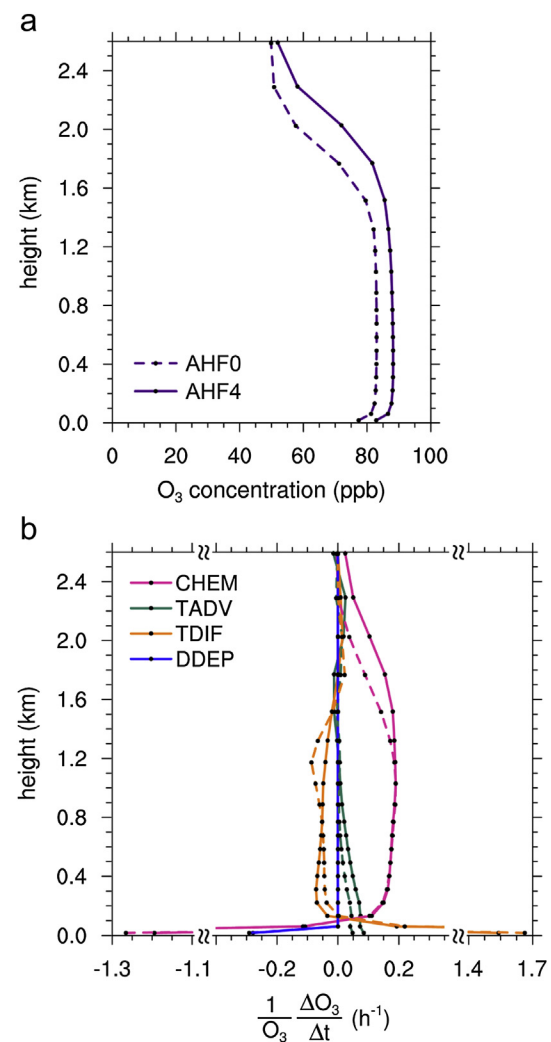


Fig. 6. Same as Fig. 5 but for the period of 1100–1500 LT 24 June 2010.

In addition to the enhanced net chemical production of O_3 in the deepened ABL, local circulation modified by anthropogenic heat can influence O_3 concentration. As an example, Fig. 7 shows the horizontal distributions of O_3 concentration and wind at 1500 LT in the AHF0, AHF1, AHF2, and AHF4 simulations. It is seen that O_3 in the surroundings is advected over the urban area by the urban breeze in the daytime similar to that in the nighttime. This advection effect is also seen in Fig. 6b, which shows relatively large positive contributions of the advection process in the lower ABL in both the AHF0 and AHF4 simulations. The contribution of the advection process in the lower ABL is larger in the AHF4 simulation than in the AHF0 simulation (Fig. 6b). Since the larger temperature difference between the urban area and surroundings in the AHF4 simulation induces a stronger urban-breeze circulation, the advection of O_3 from the surroundings is enhanced in the AHF4 simulation (e.g., compare Fig. 7a with d).

Even though the amount of O_3 advected by the urban breeze seems to largely depend on the intensity of urban-breeze circulation (Fig. 7), the difference in contribution of the advection

process between the AHF0 and AHF4 simulations in Fig. 6b is relatively small. This feature arises because anthropogenic heat also modifies the sea breeze. The larger temperature difference between the urban area and the sea owing to the stronger anthropogenic heat accelerates the inland penetration of the sea breeze and increases sea breeze intensity (Fig. 7). It is seen that O_3 concentration is low behind the sea-breeze front in the urban area where NO_x emissions are high (e.g., the southwestern region outside Seoul and the southwestern region of Seoul). In the sea-breeze inflow layer that is shallower than the urban boundary layer, O_3 concentration significantly decreases due to NO_x titration in the regions where NO_x emissions are high. Therefore, the concentration of O_3 brought into the urban area by the sea breeze from the NO_x source regions is low. Because the contributions of the advection process associated with the urban breeze and the sea breeze are opposite to each other, the net contribution of the advection process averaged over the urban analysis area is small (Fig. 6b).

It is interesting to note that O_3 concentration over the sea is different depending on anthropogenic heat intensity (see Fig. 7). As

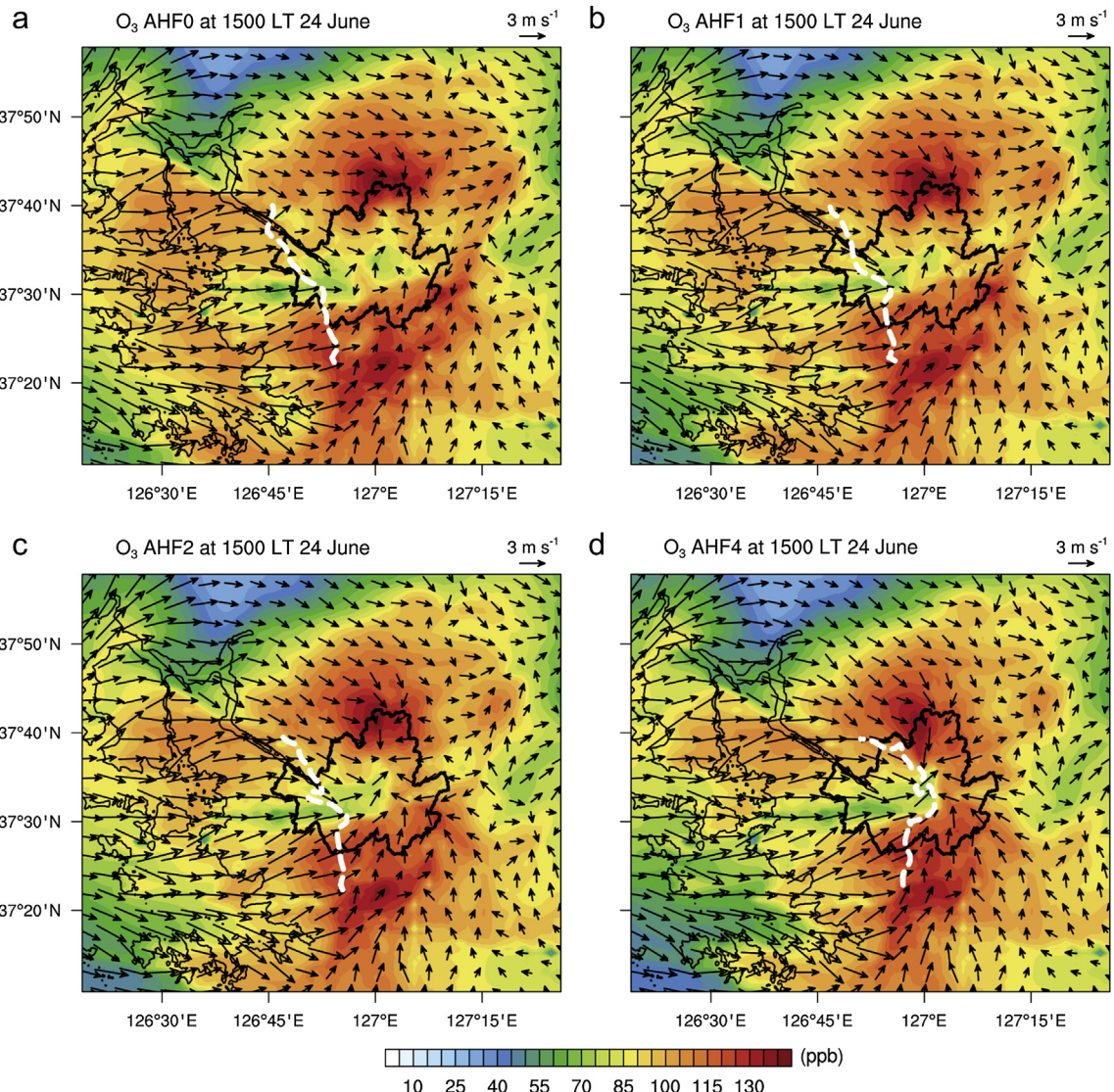


Fig. 7. Horizontal distributions of O_3 concentration and wind at the lowest model level at 1500 LT 24 June 2010 in the (a) AHF0, (b) AHF1, (c) AHF2, and (d) AHF4 simulations. The white-dashed lines in (a)–(d) indicate rough locations of sea-breeze front in the four simulations.

mentioned above, in the nighttime, the advection of NO_x over the sea is enhanced in the AHFO simulation in which the weakest urban breeze develops. Thus, in the AHFO simulation, O_3 production over the sea is enhanced in the daytime and the advection of O_3 by the sea breeze in the daytime increases O_3 concentration in the urban area. Because of the advection, O_3 concentration in the early evening in the AHFO simulation becomes higher than that in the AHF4 simulation (Fig. 3a).

It is shown that due to anthropogenic heat the chemical production of O_3 is enhanced in the modified boundary layer. The chemical production of O_3 can also be enhanced by the modified local circulation, i.e., the urban-breeze circulation, as demonstrated in Ryu et al. (2013). Fig. 8 shows the ABL-averaged contributions of the chemical process obtained from the IPR analysis at 1500 LT in the AHFO and AHF4 simulations. The enhanced chemical production of O_3 over the sea or the western region of

the domain in the AHFO simulation is also confirmed by comparing Fig. 8a with b. In both simulations, the net chemical production of O_3 is small in the regions where NO_x emissions are high, such as the southwestern region outside Seoul and the southwestern region of Seoul. Moreover, the sign of the net chemical production of O_3 is negative in some regions. On the other hand, in both simulations, the net chemical production of O_3 in the surroundings is large. This is due to high biogenic volatile organic compound (BVOC) emissions and very low NO_x emissions in the surroundings. Note that there are large forest areas near Seoul to the north, east, and south, and that BVOCs can be emitted substantially from these forest areas. It is interesting that the chemical production of O_3 is also enhanced in the regions where the urban breeze prevails. Because the urban breeze in the AHF4 simulation is stronger, the chemical production of O_3 in Seoul is more enhanced in the AHF4 simulation. It is also found that in the regions where the urban breeze prevails the ratio of the rate of formation of peroxides divided by the rate of formation of HNO_3 (the ratio suggested by Sillman (1999)) increases in the AHF4 simulation and the rate of reaction between OH and NO_2 is reduced in the AHF4 simulation as compared with the results of the AHFO simulation (not shown). This also suggests the enhanced chemical production of O_3 in the regions where the urban breeze prevails.

To find out the reasons for the enhanced chemical production of O_3 in the regions under the influence of the urban-breeze circulation, the vertical cross sections of O_3 and isoprene concentrations and wind at 1500 LT along the line A–B (shown in Fig. 1b) are presented in Fig. 9. As can also be seen in Figs. 6 and 7, O_3 is advected over the urban area from the surroundings following the urban breeze in both the AHFO and AHF4 simulations (Fig. 9). Because of the stronger urban breeze in the AHF4 simulation, the advection of O_3 is more significant and O_3 concentration in the urban area is higher in the AHF4 simulation. As a reason for the enhanced chemical production of O_3 in the AHF4 simulation, one may expect that the advection of isoprene that is one of the important BVOC species for O_3 production is responsible for the enhanced chemical production of O_3 . However, the isoprene concentration fields in both simulations do not seem to support this expectation (Fig. 9c and d). Rather, the isoprene concentration is lower in the AHF4 simulation.

To examine in more detail how the urban breeze influences the chemical production of O_3 , an Integrated Reaction Rate (IRR) analysis (Gipson, 1999) is performed as done in Ryu et al. (2013). Fig. 10a and b show the rate of reaction between OH and isoprene at 1500 LT along the line A–B in the AHFO and AHF4 simulations. Clearly, the rate of reaction between OH and isoprene in both simulations is high in the regions where the isoprene is emitted. Since isoprene can be advected to some extent by the urban breeze, the enhanced rate of reaction between OH and isoprene is found in Fig. 10b ($\sim 37^{\circ}40'\text{N}$). However, this enhancement does not directly correspond to the enhanced rate of reactions between OH and volatile organic compounds (VOCs) (Fig. 10f) that is linked closely to the enhanced chemical production of O_3 (not shown). Fig. 10c and d show the enhanced rate of reactions between OH and oxygenated VOCs (OVOCs) in both simulations in the regions where the urban breeze prevails. These results suggest that the advection of the oxidation products of isoprene (and other BVOCs as well) contributes to the enhanced chemical production of O_3 in the regions where the urban breeze prevails. The contribution of the advection of isoprene itself is small because the lifetime of isoprene is relatively short (~ 0.5 h, Carslaw et al., 2000). This finding is consistent with that of Geng et al. (2011). They suggested that the continuous oxidation of isoprene leads to the enhancement of carbonyls (such as formaldehyde and acetaldehyde) in regions downwind of forests

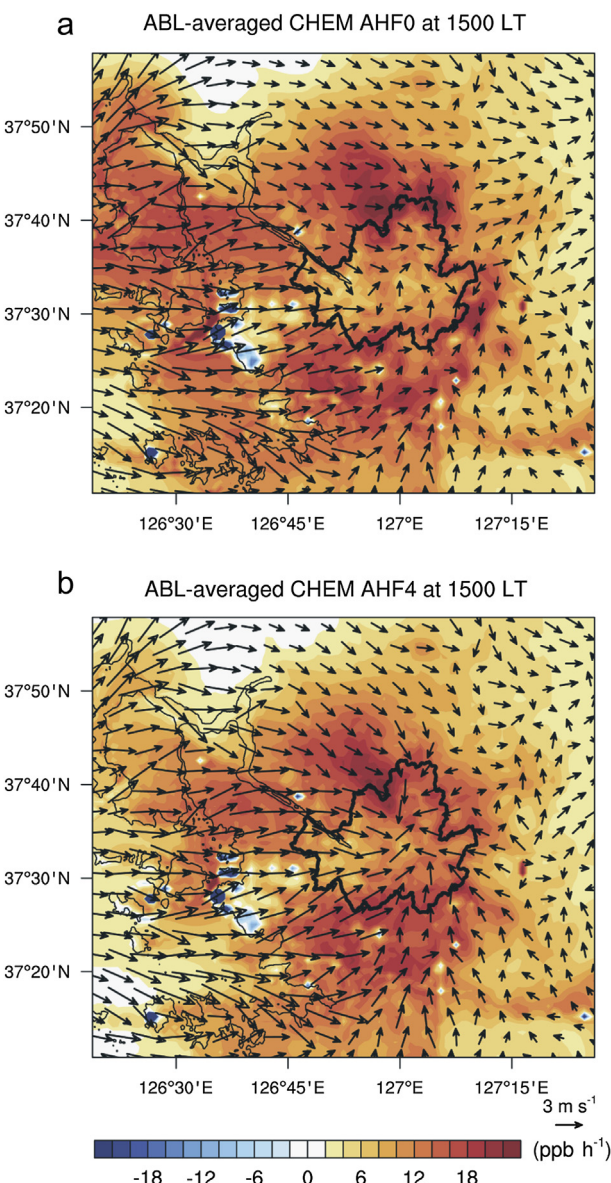


Fig. 8. Horizontal distributions of ABL-averaged contribution of the chemical process to O_3 concentration and wind at the lowest model level at 1500 LT 24 June 2010 in the (a) AHFO and (b) AHF4 simulations.

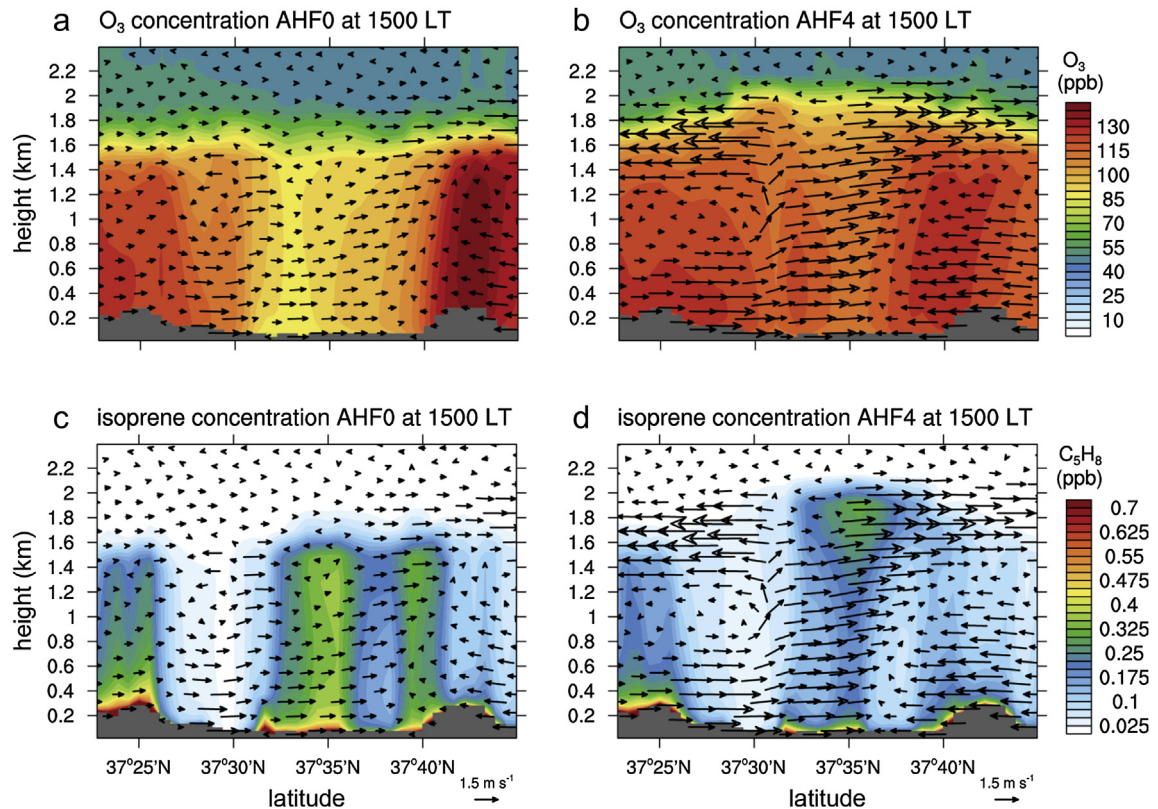


Fig. 9. Vertical cross sections of (a) O₃ concentration and wind and (c) isoprene concentration and wind along the line A–B in Fig. 1b at 1500 LT 24 June 2010 in the AHF0 simulation. (b) and (d) are the same as (a) and (c), respectively, but for the AHF4 simulation.

and that this process leads to an enhanced chemical production of O₃ in these regions.

Interestingly, the rate of reactions between OH and VOCs in the AHF0 simulation is high above the mountain that is centered near 37°42'N where the urban-breeze circulation is less prominent. This high reaction rate is linked closely to the enhanced chemical production of O₃ above the mountain, as seen in Fig. 8a. On the other hand, in the AHF4 simulation, the rate of reactions between OH and VOCs above the mountain is rather low. These results indicate that the chemical production of O₃ is enhanced in the stagnant air mass in the surroundings where BVOC emissions are high. Because the urban-breeze circulation starts to develop earlier and the urban-breeze circulation becomes stronger when anthropogenic heat intensity is stronger (e.g., AHF4 simulation), there is little time for the enhanced chemical production of O₃ and the accumulation of O₃ in the air mass in the surroundings. When anthropogenic heat is weak or absent, the development of urban-breeze circulation is delayed and the urban-breeze circulation prevails later (in the late afternoon or early evening). Thus, the O₃-rich air is advected over the urban area in the late afternoon or early evening. This advection effect also causes the O₃ concentration in the early evening to be higher in the AHF0 simulation than in the AHF4 simulation (Fig. 3a). As mentioned previously, another reason for the higher O₃ concentration in the AHF0 simulation in the early evening is the advection of the O₃-rich air from the sea by the sea breeze.

4. Summary and conclusions

The effects of anthropogenic heat on ozone air quality under fair weather conditions in the Seoul metropolitan area were examined

using the WRF-CMAQ model. The release of anthropogenic heat was found to increase O₃ concentration in the urban area, and the degree of the effect was found to increase as anthropogenic heat intensity increases. The increase in O₃ concentration is larger in the nighttime than in the daytime because the chemical loss of O₃ by the reaction with NO is more reduced in the nighttime due to the large dilution of NO_x in the deepened urban boundary layer. In the daytime, in addition to the dilution effect associated with the modified boundary layer, the urban-breeze circulation modified by anthropogenic heat was found to contribute to an increase in O₃ concentration in the urban area. In this study area, O₃ concentration is high in the surroundings where BVOC emissions are high. Because the urban-breeze circulation becomes stronger as anthropogenic heat intensity increases, the amount of O₃ advected over the urban area from the surroundings increases. In addition to the direct advection of O₃, the advection of oxidant products of BVOCs by the urban breeze from the surroundings results in an enhanced chemical production of O₃ in the urban area. Meanwhile, the inland penetration of the sea breeze is accelerated due to anthropogenic heat. Because the chemical loss of O₃ by NO in the relatively shallow sea-breeze inflow layer is enhanced in the regions where NO_x emissions are high, the modified sea breeze acts to decrease the O₃ concentration in the urban area in the late afternoon and early evening.

In the present study, the effects of anthropogenic heat on ozone air quality for the particular summertime case were examined. The effects of anthropogenic heat could be different depending on the season. Also, the effects of anthropogenic heat on some other air pollutants (e.g., particulate matters) might be different from those on ozone. Thus, further related studies would be desired.

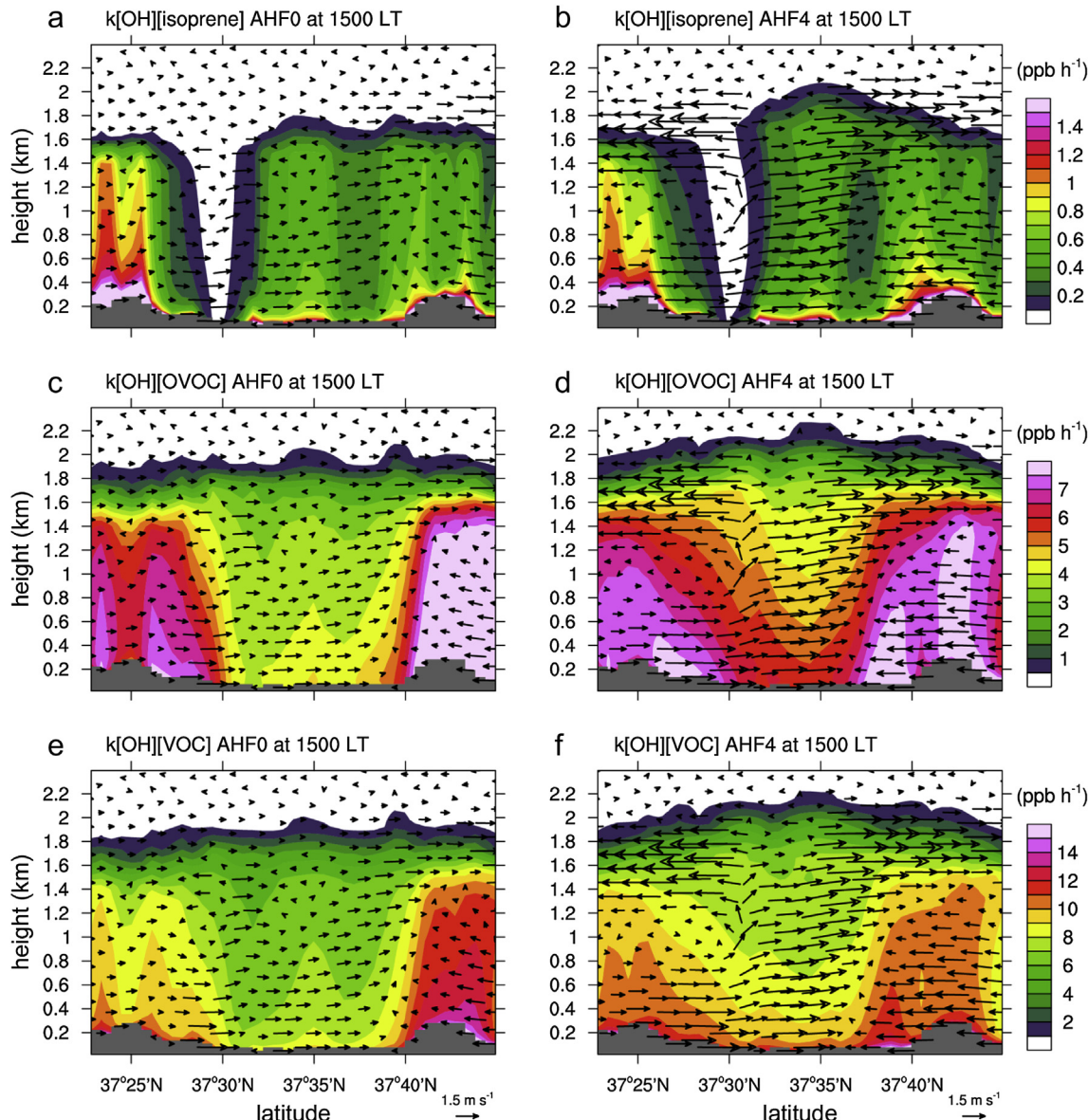


Fig. 10. Vertical cross sections of (a) rate of reaction between OH and isoprene and wind, (c) rate of reactions between OH and OVOCs and wind, and (e) rate of reactions between OH and VOCs and wind along the line A–B in Fig. 1b at 1500 LT 24 June 2010 in the AHF0 simulation. (b), (d), and (f) are the same as (a), (c), and (e), respectively, but for the AHF4 simulation.

Acknowledgments

The authors thank an anonymous reviewer for providing valuable comments on this work. This work was supported by the National Research Foundation of Korea (NRF) grant funded by the Korea Ministry of Education, Science and Technology (MEST) (No. 2012-0005674).

References

- Carslaw, N., Bell, N., Lewis, A.C., McQuaid, J.B., Pilling, M.J., 2000. A detailed case study of isoprene chemistry during the EASE96 Mace Head campaign. *Atmospheric Environment* 34, 2827–2836.
- Chen, Y., Jiang, W.M., Zhang, N., He, X.F., Zhou, R.W., 2009. Numerical simulation of the anthropogenic heat effect on urban boundary layer structure. *Theoretical and Applied Climatology* 97, 123–134.
- Fan, H., Sailor, D.J., 2005. Modeling the impacts of anthropogenic heating on the urban climate of Philadelphia: a comparison of implementations in two PBL schemes. *Atmospheric Environment* 39, 73–84.
- Geng, F., Tie, X., Guenther, A., Li, G., Cao, J., Harley, P., 2011. Effect of isoprene emissions from major forests on ozone formation in the city of Shanghai, China. *Atmospheric Chemistry and Physics* 11, 10449–10459.
- Gipson, G.L., 1999. Science Algorithms of the EPA Models-3 Community Multiscale Air Quality (CMAQ) Modeling System: Process Analysis. EPA/600/R-99/030. US EPA, p. 37. Online available at: <http://www.epa.gov/asmdnerl/CMAQ/ch16.pdf>.
- Ichinose, T., Shimodozo, K., Hanaki, K., 1999. Impact of anthropogenic heat on urban climate in Tokyo. *Atmospheric Environment* 33, 3897–3909.
- Kondo, H., Kikegawa, Y., 2003. Temperature variation in the urban canopy with anthropogenic energy use. *Pure and Applied Geophysics* 160, 317–324.
- Lee, S.-H., Song, C.-K., Baik, J.-J., Park, S.-U., 2009. Estimation of anthropogenic heat emission in the Gyeong-In region of Korea. *Theoretical and Applied Climatology* 96, 291–303.
- Lin, C.-Y., Chen, F., Huang, J.C., Chen, W.-C., Liou, Y.-A., Chen, W.-N., Liu, S.-C., 2008. Urban heat island effect and its impact on boundary layer development and land–sea circulation over northern Taiwan. *Atmospheric Environment* 42, 5635–5649.
- Makar, P.A., Gravel, S., Chirkov, V., Strawbridge, K.B., Froude, F., Arnold, J., Brook, J., 2006. Heat flux, urban properties, and regional weather. *Atmospheric Environment* 40, 2750–2766.
- Ohashi, Y., Genchi, Y., Kondo, H., Kikegawa, Y., Yoshikado, H., Hirano, Y., 2007. Influence of air-conditioning waste heat on air temperature in Tokyo during summer: numerical experiments using an urban canopy model coupled with a building energy model. *Journal of Applied Meteorology and Climatology* 46, 66–81.

- Oke, T.R., Johnson, G.T., Steyn, D.G., Watson, I.D., 1991. Simulation of surface urban heat islands under 'ideal' conditions at night part 2: diagnosis of causation. *Boundary-Layer Meteorology* 56, 339–358.
- Ryu, Y.-H., Baik, J.-J., Lee, S.-H., 2011. A new single-layer urban canopy model for use in mesoscale atmospheric models. *Journal of Applied Meteorology and Climatology* 50, 1773–1794.
- Ryu, Y.-H., Baik, J.-J., Kwak, K.-H., Kim, S., Moon, N., 2013. Impacts of urban land-surface forcing on ozone air quality in the Seoul metropolitan area. *Atmospheric Chemistry and Physics* 13, 2177–2194.
- Ryu, Y.-H., Baik, J.-J., 2013. Daytime local circulations and their interactions in the Seoul metropolitan area. *Journal of Applied Meteorology and Climatology* 52, 784–801.
- Sailor, D.J., Lu, L., 2004. A top-down methodology for developing diurnal and seasonal anthropogenic heating profiles for urban areas. *Atmospheric Environment* 38, 2737–2748.
- Sang, J., Liu, H., Liu, H., Zhang, Z., 2000. Observational and numerical studies of wintertime urban boundary layer. *Journal of Wind Engineering and Industrial Aerodynamics* 87, 243–258.
- Sarrat, C., Lemonsu, A., Masson, V., Guedalia, D., 2006. Impact of urban heat island on regional atmospheric pollution. *Atmospheric Environment* 40, 1743–1758.
- Sillman, S., 1999. The relation between ozone, NO_x and hydrocarbons in urban and polluted rural environments. *Atmospheric Environment* 33, 1821–1845.